Accepted Manuscript

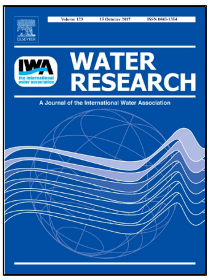

Comparative power demand of mechanical and aeration imposed shear in an immersed membrane bioreactor

P. Buzatu, M.S. Nasser, H. Qiblawey, S. Judd

PII:	S0043-1354(17)30779-0
DOI:	10.1016/j.watres.2017.09.024
Reference:	WR 13218
To appear in:	*Water Research*
Received Date:	31 May 2017
Revised Date:	09 September 2017
Accepted Date:	12 September 2017

Please cite this article as: P. Buzatu, M.S. Nasser, H. Qiblawey, S. Judd, Comparative power demand of mechanical and aeration imposed shear in an immersed membrane bioreactor, *Water Research* (2017), doi: 10.1016/j.watres.2017.09.024

Comparative energy demand of mechanical and aeration imposed shear in an MBR

Highlights

Mechanical and aeration-imposed shear in an immersed membrane bioreactor compared

Sludge rheology encompassed using literature viscosity (η) vs shear (γ) relationships

Specific power demand determined as a function of γ for both systems

Power demand for mechanical shear 20-70% less than that of conventional air scouring

Absolute power demand strongly dependent on sludge rheological properties (η vs. γ)

Water Research, 2017, Volume 126, 1 December 2017, Pages 208-215
DOI:10.1016/j.watres.2017.09.024

Comparative power demand of mechanical and aeration imposed shear in an immersed membrane bioreactor

P. Buzatu[1], M. S. Nasser[1], H. Qiblawey[2], and S. Judd[1,3*]
[1]Gas Processing Center, Qatar University
[2]Department of Chemical Engineering, Qatar University
[3]Cranfield Water Science Institute, Cranfield University
*Corresponding author, simon.judd@qu.edu.qa

Abstract

The power demanded for the application of mechanically-imposed shear on an immersed flat sheet (iFS) membrane bioreactor (MBR) has been compared to that of conventional membrane air scouring. Literature correlations based on the Ostwald model were used to define the rheological characteristics of an MBR sludge. The correlation of specific power demand ($\overline{P'}$, in Watts per m^2 membrane area) with shear rate γ in s^{-1} was developed from first principles through a consideration of the force balance on the system in the case of mechanically-imposed shear. The corresponding aeration imposed shear correlation was interpreted from literature information.

The analysis revealed the energy required to impose a shear mechanically through oscillation (or reciprocation) of the membrane to be between 20 and 70% less than that demanded for providing the same shear by conventional aeration of the immersed membrane. The energy saving increases with decreasing shear in accordance with a power demand ratio (aeration:mechanical) of $1400\gamma^{-1.4}$ for a specific sludge rheology. Whilst the absolute $\overline{P'}$ value is dependent on the sludge rheology, the aeration:mechanical power demand ratio is determined by the difference in the two exponents in the respective correlations between $\overline{P'}$ and γ. Consequently, aeration-imparted shear becomes energetically favoured beyond some threshold shear rate value (~180 s^{-1}, based on the boundary conditions applied in the current study). The

outcomes qualitatively corroborate findings from the limited practical measurement of energy demand in MBRs fitted with reciprocating immersed membranes.

Keywords *Membrane bioreactor; Mechanical shear; Membrane aeration; Sludge rheology; Power; Flat sheet*

Notation

a,**b**,**c**,**d**		Empirical constants in general Ostwald equation (Equation 1)
$\vec{a}$		Linear acceleration of the membrane, m·s^{-2}
A		Area of one side of membrane panel, m^{-2}
A_x		Cross-sectional area of membrane channel, m^{-2}
C_d		Drag coefficient, -
$C_{f,z}$		Skin friction coefficient, -
E'_A		Specific energy demand for air pumping, kWh·Nm^{-3}
$\vec{F}_A$		Archimedes force, kg·m·s^{-2}
$\vec{F}_D$		Drag force, kg·m·s^{-2}
$\vec{F}_g$		Gravitational force, kg·m·s^{-2}
$\vec{F}_{pull}$		Force required to pull membrane, kg·m·s^{-2}
$\vec{F}_{push}$		Force required to push membrane, kg·m·s^{-2}
g		Gravitational acceleration, m·s^{-2}
h		Height of sludge above rising air bubble, m
J		Operating flux, L·m^{-2}·h^{-1}
k		General constant, kWh·bar^{-1}·m^{-3}
l		Membrane panel length, m
L		Length of rod connecting crank to membrane, m
m	exp(	**a**·$X^{\mathbf{b}}$)
M		Membrane panel mass, kg
n	**c**	·$X^{\mathbf{d}}$
P	Power, W	
$\overline{P'}$		Specific power per unit membrane area, W·m^{-2}

$p_{A,in}$	Inlet blower pressure, bar
$p_{A,out}$	Outlet blower pressure, bar
Q_A	Air flow rate, $Nm^3 \cdot h^{-1}$
r	Crank radius, m
R	Ratio of membrane channel thickness to membrane panel length, -
Re_z	Local Reynolds number, -
SAD_m	Specific aeration demand per unit membrane area, $Nm^3 \cdot m^{-2} \cdot h^{-1}$
SAD_p	Specific aeration demand per unit permeate flow, $Nm^3 \cdot m^{-3}$
SED_m	Specific energy demand of membrane permeation, $kWh \cdot m^{-3}$
T	Period of rotation, s
v	Linear velocity of membrane, $m \cdot s^{-1}$
v_a	Interstitial air velocity, $m \cdot s^{-1}$
V	Volume occupied by membrane panel, m^3
y	Position of the membrane upper edge, m
X	Mixed liquor suspended solids (or sludge) concentration
z	Distance along the membrane sheet, m
γ	Shear rate, s^{-1}
δ	Membrane panel separation (or channel thickness), m
η_a	Apparent viscosity, mPa·s, or $g \cdot m^{-1} \cdot s^{-1}$
θ	Angle of rotation, rad
ξ_m	Total motor or blower efficiency, -
ρ_s	Sludge density, $kg \cdot m^{-3}$
φ	Angle between the applied force and the direction of movement, rad
ω	Angular velocity of membrane, $rad \cdot s^{-1}$

1 Introduction

The imparted shear in a membrane separation system is of fundamental importance, since it largely determines the mass transfer of water and solutes through the membrane (Rautenbach and Albrecht, 1989). Shear is most usually imposed by crossflow of the retentate along the membrane surface, as is the case for classical pumped sidestream membrane bioreactors (sMBRs), or by air bubbles, as for air-lift sidestream MBRs (A-L sMBRs) or immersed MBRs (iMBRs) (Judd, 2010).

Shear can also be imposed mechanically (Zsirai et al, 2016; Wang et al, 2014). A recent review of the literature (Zsirai et al, 2016) indicated that shear rates of 2,000 to 300,000 s^{-1} have been employed in studies of forced mechanical shear systems, such as rotating or vibrating discs, with corresponding specific energy demand for membrane permeation (SED_m) values well in excess of 1 kWh per m^3 permeate for full-scale systems. This is to be distinguished from the much lower air scour-generated shear rates of less than 2000 s^{-1} (Yang et al, 2017, 2009; Böhm and Kraume, 2015; Delgado et al, 2007; Laera et al, 2007; Pollice et al, 2006) determined or computed for iMBRs, based on immersed flat sheet (iFS) or hollow fibre (iHF) membrane configurations, or A-L sMBRs. For the immersed technologies SED_m values, encompassing energy contributions from both air scouring and permeate pumping, are generally below 0.5 kWh·m^{-3} (Judd, 2011), with the iFS configurations tending to be more energy-intensive than the iHF ones. This compares with values usually well above 1 kWh·m^{-3} for a classical pumped sidestream MBR (sMBR), although values of 0.55-0.65 kWh·m^{-3} have been reported from full-scale sidestream-configured installations for both “low-energy” pumped multi-tube and rotating disc membrane modules (Poudel, 2016; Judd, 2011, 2014).

The application of forced mechanical shear in MBRs has been reported in a number of recent studies of iHF systems (Chatzikonstantinou et al, 2016; Li et al, 2016; Ho et al, 2015ab; Qin et al, 2015; Zamani et al, 2014), and has been implemented at pilot/full scale using rotating membrane discs (Poudel, 2016; Jørgensen et al, 2014). Outcomes from recent pilot-scale studies suggest that SED_m values for vibrating or oscillating iHF systems may be as low as 0.074 $kWh \cdot m^{-3}$ if forced mechanical shear can completely displace air scour-generated shear (Ho et al, 2015ab).

Correlations between flux J and shear rate γ have been available from bench-scale iHF mechanical shear studies for over a decade (Beier et al., 2006, 2007). However, studies of energy demand for such MBR systems have been extremely limited. Indeed, actual correlation of energy demand with shear for iMBRs appears to have been restricted to a comparison of two different MBR configurations (Ratkovich et al, 2012) and a single study encompassing direct practical measurement of SED_m conducted on a mechanical shear-based iHF pilot-scale MBR (Ho et al, 2015ab). Despite the existence of at least one commercial MBR technology employing mechanical shear (Poudel, 2016), the nature of the relationship between energy (or power) demand and shear appears to have largely overlooked. Expressions reported for high-shear, high-end abiotic separations cannot be extrapolated to the much lower-shear operation of an MBR since the rheological properties of the MBR mixed liquor are very complex (Lopez et al, 2015; Ratkovich et al, 2013; Eshtiaghi et al, 2013; Pollice et al, 2006) and differ substantially from those of matrices treated by the forced shear filtration devices (Zsirai et al, 2016).

There is an obvious need to establish the true potential energy benefit of forced mechanical shear over aeration-imposed shear based on the same system configuration and prevailing conditions (Fig. 1). The analysis used in the current paper (Fig. 2) proceeds through:

Figure 1: Shear:power overall inter-relationships

Figure 2: Method of power demand determination/comparison: note that the flux inter-relationships (grey arrows) do not directly feature in the governing shear:power relationship

a) establishing the relationship between shear and aeration rate for the conventional immersed system, and then
b) determining the oscillation (or reciprocation) rate required to sustain this shear for a mechanically-imposed shear based MBR, and subsequently
c) determining the respective power requirements for both the mechanically and aeration-imposed shear systems.

Since both the shear rate and sludge rheological properties are common to both systems, the flux generated by the imposed shear can also be assumed to be common to both systems (Fig. 2). The challenge is therefore one of quantifying the power demanded for generating the same shear by the two different approaches, and then assuming that the flux:shear relationship to be common to both systems. It is on such a precept that the study is based. The approach is limited to the iFS configuration which is geometrically less complex than an iHF.

2 Theoretical development

2.1 Sludge rheology

A critical component of the determination of energy demand is the correlation of shear with viscosity. The shear can then be imparted through aeration or mechanical agitation, either of which will demand power. A key principle of this approach is that the flux sustained relates solely to the shear itself and is independent of the means by which it is imposed.

There have been a significant number of studies of the rheological properties of activated sludge mixed liquors, including MBRs, and these have been subject to various critical reviews (Tang and Zhang, 2014; Ratkovich et al, 2013; Eshtiaghi et al, 2013). There are essentially three common algebraic forms (Bingham, Ostwald, and Herschel-Bulkley, arising from different assumptions) which have been used to define the relationship between the apparent viscosity η_a in mPa·s, the sludge (or mixed liquor) solids concentration X in g·L^{-1} and the applied shear rate γ in s^{-1}. Of these three the Ostwald model has often been used:

$$\eta_a = \exp\left(\mathbf{a}X^{\mathbf{b}}\right)\gamma^{\mathbf{c}X^{\mathbf{d}}} \quad (1)$$

where the **a-d** are empirical constants which have been defined by various workers (Table 1).

Table 1: Published values of empirical constants for Equation 1

Equation (1) can thus be used to determine the apparent viscosity η_a for an applied shear rate γ for a given mixed liquor suspended solids (MLSS), or sludge, concentration X(Fig. 3), the shear being generated either by aeration or mechanically. X is generally between 3 and 4 g·L^{-1} for conventional activated sludge processes and 9-15 g·L^{-1} for MBRs.

Figure 3: Apparent viscosity η_a vs. shear rate γ according to the four Ostwald-based expressions based on Equation 1

2.2 Aeration-imposed system

The power P dissipated by bubbles rising in the stagnant sludge suspension through the displacement of the liquid ahead of them is given by (Logan, 1999):

$$P = \rho_s \cdot Q_A \cdot g \cdot h \quad (2)$$

where Q_A is the air flow-rate, ρ_s the sludge density, g the gravity constant and h is the height of the liquid phase covered by the bubbles. A number of expressions have been presented

quantifying the average shear associated with the movement of air bubbles (Sanchez et al, 2006), amongst the simplest being (Delgado et al, 2008):

$$\gamma = \left(\frac{\rho_s \cdot Q_A \cdot g}{A_x \cdot \eta_a} \right)^{0.5} \quad (3)$$

where A_x is the cross-sectional air sparging area, which for an iFS membrane module is the interstitial gap between the membrane plates. If the channel thickness is δ, the membrane module height l and the membrane surface area for one panel side is A, then:

$$A_x = \frac{2 \cdot \delta \cdot A}{l} = 2 \cdot R \cdot A \quad (4)$$

where $R = \delta/l$. Substituting this into Equation (3) and noting that $Q_A/A = SAD_m$, the specific aeration demand per unit area in $Nm^3 \cdot m^{-2} \cdot h^{-1}$ is:

$$\gamma = \left(\frac{\rho_s \cdot SAD_m \cdot g}{2 \cdot 3600 \cdot R \cdot \eta_a} \right)^{0.5} \quad (5)$$

where the $\gamma : \eta_a$ relationship is determined by the empirical constant values in Equation (1) (Table 1, Fig. 3), such that:

$$\gamma = \left(\frac{\rho_s \cdot SAD_m \cdot g}{7200 \cdot R \cdot m} \right)^{\frac{1}{2+n}} \quad (6)$$

where $m = \exp(\mathbf{a} \cdot X^{\mathbf{b}})$ and $n = \mathbf{c} \cdot X^{\mathbf{d}}$, **a**-**d** being as previously defined (Table 1). The SAD_m thus imparts a γ value dependent on both the solids concentration and bulk sludge rheology.

SAD_m values employed in full-scale iFS MBRs typically range from 0.3 to 0.75 $Nm^3 \cdot m^{-2} \cdot h^{-1}$ (Judd, 2011, 2014). This equates to an interstitial air velocity ($v_a = Q_A/A_x = 2 \cdot l \cdot SAD_m/\delta$) of ~0.03-0.07 $m \cdot s^{-1}$ based on a typical channel width of 6 mm and a membrane length of 1 m, at the low end of air velocity values measured or generally employed in MBR rheological and/or modelling studies (Table 2). According to the four expressions listed in Table 1, within the stated operational envelope of 0.3-0.75 $Nm^3 \cdot m^{-2} \cdot h^{-1}$ SAD_m the corresponding range of γ is 82-

265 s^{-1} at a typical membrane tank sludge solids concentration of 12 $g \cdot L^{-1}$ and assumed density 1100 $kg \cdot m^{-3}$ (Fig. 4). This γ range is also within the wide range of published γ values (Table 2).

Table 2: Published values of shear rate and interstitial air velocities for iMBRs

The aeration energy in kWh per Nm^3 of air delivered, or the power per unit air flow (i.e. P/Q_A) is defined as (Judd, 2014):

$$E_A^{'} = k \cdot p_{A,in} \cdot \left[\left(\frac{p_{A,out}}{p_{A,in}} \right)^{0.283} - 1 \right] \quad (7)$$

Figure 4: Shear rate generated at increasing SAD_m values and two different MLSS concentrations, according to four Ostwald-based expressions given in Table 1

where $p_{A,in}$ and $p_{A,out}$ are respectively the blower inlet and outlet pressures, the difference being largely determined by the hydrostatic head produced by the depth of submersion of the aerator. k is a constant for a specific system and is around 0.18 $kWh \cdot bar^{-1} \cdot m^{-3}$ for $E_A^{'}$ in kWh per Nm^3 and $P_{A,in}$ in bar (Judd, 2014), based on a blower efficiency of 60%. For an aerator submerged to a 5 m depth the outlet:inlet pressure ratio is 1.5, giving an $E_A^{'}$ value of ~0.022 $kWh \cdot Nm^{-3}$. The SED_m is then given by:

$$SED_m = E_A^{'} \cdot \frac{SAD_m}{J} \quad (8)$$

where J is the flux in units of $m \cdot h^{-1}$ (10^{-3} $L \cdot m^{-2} \cdot h^{-1}$ or LMH) and SAD_m/J equates to SAD_p, the (unitless) specific aeration demand in Nm^3 air applied per m^3 permeate delivered. It then follows that the specific power $\overline{P^{'}}$ in W per m^2 membrane area is:

$$\overline{P^{'}} = 10^3 \cdot E_A^{'} \cdot SAD_m \approx 22 \cdot SAD_m \quad (9)$$

Thus, for SAD_m ranging from 0.3-0.75 $Nm^3 \cdot m^{-2} \cdot h^{-1}$ $\overline{P'}$ is within the range of 7-17 $W \cdot m^{-2}$ membrane area and is associated with the previously determined shear rate γ of 82-265 s^{-1}. Values tend towards the lower end of the SAD_m range for double-deck iFS membrane modules where SAD_m is halved since the same volume of air scours double the membrane area compared with a single deck (Judd, 2010). Appropriate flux values for determining *SED* from Equation (8) can be informed from full-scale plant. Municipal MBR plants tend to operate at between 20 and 25 LMH net flux (Judd, 2010, 2014), yielding *SED* values of 0.26-0.83 $kWh \cdot m^{-3}$ - again tending towards the lower end of this range for stacked modules.

2.3 Mechanically-imposed shear

An appropriate arrangement for a mechanical process is a simple crank and arm (Fig. 5a) moving the membrane panel vertically (Fig. 5b). The motor power required to vertically displace the panel via the crank can be derived via a first-principles mathematical model. The model proceeds via definition of the vector forces acting on the membrane and a balance produced for the separate pushing and pulling parts of the membrane reciprocation.

The forces acting on the moving membrane panel (Fig. 5b) are:

- the gravitational force – the product of the mass of the panel, M, and the gravitational acceleration, g:

$$\vec{F}_g = M \cdot \vec{g} \tag{10}$$

- the upward buoyant force given by the product between weight of the fluid that the body displaces and the gravitational acceleration:

$$\vec{F}_A = V \cdot \rho_s \cdot \vec{g} \tag{11}$$

where V is the volume in sludge occupied by a membrane panel, ρ_s the density of the activated sludge and g the gravitational acceleration;

- the drag, $\vec{F}_D$, is the force acting opposite to the relative motion of an object moving through a surrounding fluid:

$$\vec{F}_D = \frac{1}{2} \cdot C_d \cdot \rho_s \cdot 2A \cdot \vec{v}^2 \tag{12}$$

where C_d is the drag coefficient, ρ_s the density of the activated sludge, A the membrane area for one side of the panel, as before, and $\vec{v}$ the directional velocity of the membrane.

Figure 5: (a) Geometric layout of the crank and arm, and (b) Forces at work in system

The skin friction coefficient $C_{f,z}$ as a function of z, the distance along the membrane sheet, is given by the Blasius solution to the boundary layer on a flat plate:

$$C_{f,z} = \frac{0.664}{\sqrt{\mathrm{Re}_z}} \tag{13}$$

where Re_z is the local Reynolds number:

$$\mathrm{Re}_z = \frac{v \cdot z \cdot \rho_s}{\eta_a} \tag{14}$$

η_a being the sludge apparent viscosity, as before. In this case the drag coefficient appearing in Equation (12) is given by the integrated skin friction coefficient over the entire length of the plate, based on laminar flow:

$$C_d = \frac{1}{l} \cdot \int_0^l \frac{0.664}{\sqrt{\mathrm{Re}_z}} \cdot dz = \frac{1.328}{\mathrm{Re}_l} \tag{15}$$

When the membrane is pulled towards the surface of the liquid, the forces balance reads:

$$-\vec{F}_{pull} - \vec{F}_A + \vec{F}_g + \vec{F}_D = -M \cdot \vec{a} \tag{16}$$

where $\vec{F}_{pull}$ is the force that must be applied to pull the membrane at a certain acceleration, $\vec{a}$.

Inserting Equations (10)-(12) into (16) and rearranging the terms leads to the following expression for the force required to pull the membrane upwards:

$$\vec{F}_{pull} = M \cdot \vec{g} + \frac{1}{2} \cdot C_d \cdot \rho_s \cdot 2A \cdot \vec{v}^2 - V \cdot \rho_s \cdot \vec{g} + M \cdot \vec{a} \tag{17}$$

When the membrane is pushed downwards, the forces balance reads:

$$\vec{F}_{push} - \vec{F}_A + \vec{F}_g - \vec{F}_D = M \cdot \vec{a} \tag{18}$$

where $\vec{F}_{push}$ is the force that must be applied to push the membrane at acceleration $\vec{a}$. Inserting Equations (10)-(12) into (18) and rearranging the terms leads to the following expression for the force required to move the membrane panel downwards:

$$\vec{F}_{push} = -M \cdot \vec{g} + \frac{1}{2} \cdot C_d \cdot \rho_s \cdot 2A \cdot \vec{v}^2 + V \cdot \rho_s \cdot \vec{g} + M \cdot \vec{a} \tag{19}$$

The work done per unit time (i.e. the instantaneous power P) is the scalar product of the applied force $\vec{F}$ (push or pull) and the linear velocity $\vec{v}$:

$$P = \vec{F} \cdot \vec{v} = F \cdot v \cdot \cos\varphi \tag{20}$$

where φ is the angle between the resulting force and the direction of movement. The power averaged over one full rotation can then be determined as the integral of the instantaneous power, divided by the period of rotation T:

$$\overline{P} = \frac{1}{T} \cdot \int_0^T P(t) \cdot dt \tag{21}$$

Substituting the force components $\vec{F}_{pull}$ and $\vec{F}_{push}$, respectively given in Equations (17) and (19), for $\overline{P}$ in the above equation and accounting for efficiency losses through the overall motor efficiency, ξ_m, the specific power per unit membrane area becomes:

$$\overline{P'} = \frac{1}{2A} \cdot \frac{1}{T \cdot \xi_m} \cdot \int_0^T \left[\left| \vec{F}_{pull}(t) \right| + \left| \vec{F}_{push}(t) \right| \right] \cdot v(t) \cdot \cos\varphi(t) \cdot dt \tag{22}$$

The specific energy demand, *SED*, required for one full up-down movement is then obtained by dividing the specific power $\overline{P'}$ by the flow $J \cdot A$.

303

304 The reciprocating motion of the membrane panel is most simply achieved via a rotating crank
305 of radius r at the top of the panel to which the panel is attached by a rod of length L (Fig. 2a),
306 the membrane being driven with the uniform angular velocity ω. Solution of Equations (17)
307 and (19) demands an expression for the acceleration $\vec{a}$, which is obtained through differentiation
308 of the equation for velocity v. This in turn is obtained through a consideration of the position of
309 the membrane's upper edge y relative to the centre of the crank, which is given by:

310 $$y = r \cdot \cos\theta + \sqrt{L^2 - \left(r \cdot \sin\theta\right)^2} \tag{23}$$

311 where θ is the angle of rotation (Fig. 2a). The velocity is obtained through differentiation of
312 Equation (23) with respect to time:

313 $$v = -r \cdot \omega \cdot \left[\sin\theta + \frac{r \cdot \sin\theta \cdot \cos\theta}{\sqrt{L^2 - \left(r \cdot \sin\theta\right)^2}} \right] \tag{24}$$

314 The acceleration a required in Equations (17) and (19) is then obtained through differentiation
315 of Equation (24):

316 $$a = -r \cdot \omega^2 \cdot \left\{ \cos\theta + \frac{\left(L/r\right)^2 \cdot \cos 2\theta + \sin^4\theta}{\left[\left(L/r\right)^2 - \sin^2\theta\right]^{3/2}} \right\} \tag{25}$$

317 The shear rate γ generated by the reciprocation of the membrane is given by the linear velocity
318 of the membrane v divided by half the separation between two membrane panels, $\delta/2$:

319 $$\gamma = \frac{2 \cdot \left|\vec{v}\right|}{\delta} \tag{26}$$

320 which in turn can be expressed as a function of the rotation speed ω as:

321 $$\gamma = \frac{2}{\delta} \cdot \left| -r \cdot \left[\sin\theta + \frac{r \cdot \sin\theta \cdot \cos\theta}{\sqrt{L^2 - \left(r \cdot \sin\theta\right)^2}} \right] \right| \cdot \omega \tag{27}$$

3 Discussion

According to the analysis undertaken, the range of shear rate γ generated through air-scouring of an iFS MBR membrane is in the range of 82-265 s^{-1}, the value depending on the sludge rheological behaviour (Equation (1) and Table 1), for SAD_m values ranging from 0.3 to 0.75 $Nm^3 \cdot m^{-2} \cdot h^{-1}$ with a corresponding interstitial air velocity of ~0.03-0.07 $m \cdot s^{-1}$. If the expression provided by Rosenberger et al (2002) is used to define the rheology, then the shear range applicable for this SAD_m range is from 82 to 155 s^{-1}. Assuming a blower efficiency of 60% and an MLSS of 12 $g \cdot L^{-1}$ the power demanded to generate this shear through aeration increases from 6.6 to 17 $W \cdot m^{-2}$ membrane area as a function of the shear rate:

$$\overline{P'} = 0.011 \cdot \gamma^{1.45} \quad (28)$$

For a typical flux of 25 LMH the corresponding SED_m is between 0.25 and 0.66 $kWh \cdot m^{-3}$, which is in reasonable agreement with the range of energy demand figures reported for air scouring of full-scale plants based on iFS membranes (Judd, 2011). This would appear to validate the use of the Rosenberger et al expression to represent the sludge rheology. Further corroborartion of this expression has been provided by the exhaustive study of Lopez et al (2015), who took sludge samples from across both industrial and municipal MBR installations at 21 different locations and MLSS concentrations ranging from 2.8 to 32 g/L.

If the same shear is generated mechanically by moving the membranes vertically using a simple cam system then, according to Equation (22), the power demanded based on a 60% overall motor efficiency is in the range 2.0 to 13 $W \cdot m^{-2}$ and can be fitted to ($R^2 = 0.998$):

$$\overline{P'} = 7.83 \cdot 10^{-6} \cdot \gamma^{2.85} \quad (29)$$

Thus, within this range of operation, mechanical application using the simple crank system appears to be between 20% and 70% more energy efficient than conventional air scouring, or 3.4-5.3 $W \cdot m^{-2}$ in absolute terms, the energy benefit being highly sensitive to the shear rate (Fig. 6). This sensitivity arises from the very significant difference in the form of the mathematical relationship between aeration and mechanically-imposed shear, most ostensibly the exponent values. The specific power ratio between the aeration and mechanical systems roughly follows a $1400\gamma^{-1.4}$ relationship, based on Equations (28) and (29). Thus, above a shear rate of ~180 s^{-1} aeration-induced shear becomes more energetically efficient.

Figure 6: vs. $\overline{P'}$ γ for aeration and mechanically imparted shear, based on an MLSS concentration of 12 $g \cdot L^{-1}$ and 60% efficiency for both the air blower and the crank motor: operational envelope indicated.

Energy correlations for an aerated and mechanically-moved MBR membrane have been reported for the immersed hollow fibre (iHF) membrane configuration (Ho et al, 2015ab). Outputs from the reciprocating iHF MBR were compared with those measured for a conventional air-scoured system operating under otherwise similar conditions with reference to mixed liquor characteristics and concentration, cleaning protocols and transmembrane pressure range. According to this study (Table 3) the specific power $\overline{P'}$ in W per unit m^2 membrane area was in the region of 1.5 $W \cdot m^{-2}$ when corrected for an optimum gear motor efficiency of 70% and a variable frequency drive (VFD) unit efficiency of 74%. This $\overline{P'}$ figure compared favourably to a corresponding figure of ~2.6 $W \cdot m^{-2}$ for the aerated membrane. The reported $\overline{P'}$ values are below the range determined for the current study since the trials were based on an iHF technology for which the aeration demand is lower (Judd, 2011); in the Ho et al case the SAD_m applied for the aerated system was 0.2 $Nm^3 \cdot m^{-2} \cdot h^{-1}$, equating to a shear of 30-42 s^{-1} depending on the assumed sludge rheology.

374**Table 3:** Operating conditions and outputs of aerated and mechanical shear comparison (Ho et al, 2015ab)

375

376 Currently, the only commercial MBR technology employing mechanical shear for MLSS
377 rejection is the Grundfos *Biobooster*, based on rotating discs. According to the scant
378 information available for a full-scale operating plant challenged with a dairy effluent feed
379 (Poudel, 2016), the specific power demand for membrane permeation is in the region of
380 22 $W \cdot m^{-2}$, equating to an SED_m of 0.63 $kWh \cdot m^{-3}$ at the average operating flux of 35 LMH
381 employed. As such the energy demand for this system is comparable to a "low energy" pumped
382 sidestream system using conventional multitube membranes (Judd, 2011).

383

384 Some key assumptions have been made in conducting the analysis. It is assumed that the
385 relationship between flux and shear rate is independent of how the shear is generated. There are
386 also necessary assumptions concerning the energetic efficiencies of both the air blower and the
387 crank motor, as well as the assumption of the validity of the Ostwald form of the apparent
388 viscosity:shear relationship (Equation (1)). However, according to the approach taken below a
389 given threshold shear value, determined by the sludge rheological behaviour, mechanically-
390 imposed shear is more energetically efficient than that imparted through conventional aeration.
391 Whilst aeration also provides bulk mixing in the membrane tank, this is to some extent obviated
392 by the pumping of the sludge through the tank at a rate 4-5 times that of the permeate flow rate
393 (which then also imparts a small amount of shear). Successful pilot-scale testing without
394 membrane air scour (Ho et al, 2015ab) suggests that this is the case.

395

396 4 Conclusions

397 The relationship between energy demand and shear has been developed for both mechanical
398 and aeration imposed shear applied to an immersed flat sheet membrane bioreactor. According

to the analysis, the energy required to impose a shear mechanically through reciprocation of the membrane is between 20% and 70% less than that required for applying the same shear by conventional aeration, the proportional energy saving increasing with decreasing shear (i.e. at lower reciprocation or aeration rates). The calculated energy demand values are significantly influenced by the rheological properties of the mixed liquor, and specifically assumptions made concerning the change in (a) the sludge viscosity, and (b) membrane flux with shear rate. However, the outputs from comparison conducted in this study can be considered valid for a single mixed liquor whose rheological behaviour can be assumed not to change according to the nature of shear imposition. The results appear to corroborate the reported energy benefit of mechanically-imposed shear from the limited practical measurements conducted on the impact of mechanical shear on energy demand for immersed MBR membranes.

Acknowledgements

This work was made possible by the support of a National Priorities Research Programme (NPRP) grant from the Qatar National Research Fund (QNRF), grant reference number NPRP8-1115-2-473. The statements made herein are solely the responsibility of the authors.

References

Beier, S.P., and Jonsson, G. (2007). Separation of enzymes and yeast cells with a vibrating hollow fiber membrane module, Sep. Purif. Technol. 53 111–118.

Beier, S.P., Guerra, M., Garde, A., and. Jonsson, G. (2006). Dynamic microfiltration with a vibrating hollow fiber membrane module: Filtration of yeast suspensions, J. Membr. Sci. 281 281–287.

Böhm, L., and Kraume, M. (2015). Fluid dynamics of bubble swarms rising in newtonian and non-newtonian liquids in flat sheet membrane systems. J. Membr. Sci., 475, 533-544.

Chatzikonstantinou, K., Tzamtzis, N., Aretakis, N., and Pappa, A. (2016). The effect of various high-frequency powerful vibration (HFPV) types on fouling control of hollow fiber membrane elements in a small pilot-scale SMBR system. Desal. Water Treat. 57(57) 27905-27913.

Delgado, S., Villarroel, R., and Gonzalez, E. (2007). Effect of the shear intensity on fouling in submerged membrane bioreactor for wastewater treatment, J. Membr. Sci. 311 (2008) 173–181.

Eshtiaghi, N., Markis, F., Yap, S. D., Baudez, J. C., and Slatter, P. (2013). Rheological characterisation of municipal sludge: A review. Water Res. 47(15) 5493-5510.

Ho, J., Smith, S., Kim, G.D., Roh, H.K. (2015a). Performance evaluation of a novel reciprocation membrane bioreactor (rMBR) for enhanced nutrient removal in wastewater treatment: A comparative study, Water Sci. Technol. 72 917-927.

Ho, J., Smith, S., Patamasank, J., Tontcheva, P., Kim, G.D., Roh, H. K (2015b). Pilot demonstration of energy-efficient membrane bioreactor (MBR) using reciprocating submerged membrane. Water Env. Res,, 87(3), 266-273.

Jørgensen, M.K., Pedersen, M.T., Christensen, M.L., and Bentzen, T.R. (2014). Dependence of shear and concentration on fouling in a membrane bioreactor with rotating membrane discs. AIChE J., 60(2), 706-715

Judd, S. (2010). The MBR Book, Butterworth-Heinemann, Oxford (2011).

Judd, S. (2014). Industrial MBRs, Judd and Judd, Cranfield, UK (2014).

Laera, G., Giordano, C., Pollice, A., Saturno, D., & Mininni, G. (2007). Membrane bioreactor sludge rheology at different solid retention times. Water Res. 41(18) 4197-4203.

Li, T., Law, A.W., Jiang, Y., Harijanto, A.K., and Fane, A.G. (2016). Fouling control of submerged hollow fibre membrane bioreactor with transverse vibration. J. Membr. Sci. 505 216-224.

Logan, B. E. (1999). Environmental Transport Processes, Wiley, NY.

Lopez J., Moreau A., Gil J.A., van der Graaf J.H.J.M., van Lier J.B., and Ratkovich N. (2015). MBR activated sludge viscosity measurement using the Delft filtration characterization method, Journal of Water Process Engineering 5 35-41.

Sánchez Pérez, J. A., Rodríguez Porcel, E. M., Casas López, J. L., Fernández Sevilla, J. M., and Chisti, Y. (2006). Shear rate in stirred tank and bubble column bioreactors. Chemical Engineering Journal 124(1-3) 1-5.

Pollice, A., Giordano, C., Laera, G., Saturno, D., and Mininni, G. (2006). Rheology of sludge in a complete retention membrane bioreactor. Environ. Technol. 27(7) 723-732.

454 Poudel, B. (2016) Membrane bioreactor (MBR) plant for treating dairy wastewater: an in-depth look at
455 the Arla milk powder factory, *The MBR Site*, accessed 26th February 2017.

456 Qin, L., Fan, Z., Xu, L., Zhang, G., Wang, G., Wu, D., Long, X., and Meng, Q. (2015). A submerged
457 membrane bioreactor with pendulum type oscillation (PTO) for oily wastewater treatment: Membrane
458 permeability and fouling control. Biores. Technol. 183 33-41.

459 Ratkovich, N., Bentzen, T. R., and Rasmussen, M. R. (2012). Energy consumption in terms of shear
460 stress for two types of membrane bioreactors used for municipal wastewater treatment processes. Arch.
461 Thermodynamics 33(2) 85-106.

462 Ratkovich, N., Horn, W., Helmus, F. P., Rosenberger, S., Naessens, W., Nopens, I., and Bentzen, T. R.
463 (2013). Activated sludge rheology: A critical review on data collection and modelling. Water Res. 47(2)
464463-482.

465 Rautenbach, R., and Albrecht, R. (1989). Membrane Processes, Wiley, Lon/NY.

466 Rosenberger, S., Kubin, K., and Kraume, M. (2002). Rheology of activated sludge in membrane
467 bioreactors, Eng. Life Sci. 2(9) 269–275.

468 Tang, B., and Zhang, Z. (2014). Essence of disposing the excess sludge and optimizing the operation of
469 wastewater treatment: Rheological behavior and microbial ecosystem. Chemosphere 105 1-13.

470 Verrecht, B., Judd, S., Guglielmi, G., Mulder, J.W., and Brepols, C. (2008). An aeration energy model
471 for an immersed membrane bioreactor, Water Res. 42 4761-4770.

472 Wang, P., Han, Y. H., Chen, J. Q., Zhang, X. F. (2014). A review of membrane separation process
473 enhanced by shearing force, Adv. Mats. Res. 1010-1012 729-732.

474 Xu, Z., and Yu, J., (2008). Hydrodynamics and mass transfer in a novel multi air lifting membrane bio
475 reactor. Chem. Eng. Sci. 63 1941–1949.

476 Yang, F., Bick, A., Shandalov, S., Brenner, A., and Oron, G. (2009). Yield stress and rheological
477 characteristics of activated sludge in an airlift membrane bioreactor. J. Membr. Sci. 334(1-2) 83-90.

478 Yang, M., Yu, D., Liu, M., Zheng, L., Zheng, X., Wei, Y., Wang, F, and Fan, Y. (2017). Optimization
479 of MBR hydrodynamics for cake layer fouling control through CFD simulation and RSM design. Biores.
480Technol. 227 102-111.

481 Zamani, F., Law, A. W. K., and Fane, A. G. (2013). Hydrodynamic analysis of vibrating hollow fibre
482membranes. J. Membr. Sci. 429 304-312.

483 Zhang, W., Peng, S., Xiao, P., He, J., Yang, P., Xu, S., & Wang, D. (2015). Understanding the evolution
484 of stratified extracellular polymeric substances in full-scale activated sludges in relation to
485 dewaterability. RSC Adv. 5(2) 1282-1294.

Zsirai, T., Qiblawey, H., Al-Marri, M., and Judd, S.J. (2016). The impact of mechanical shear on membrane flux and energy demand, J. Membrane Sci. 516 56–63.

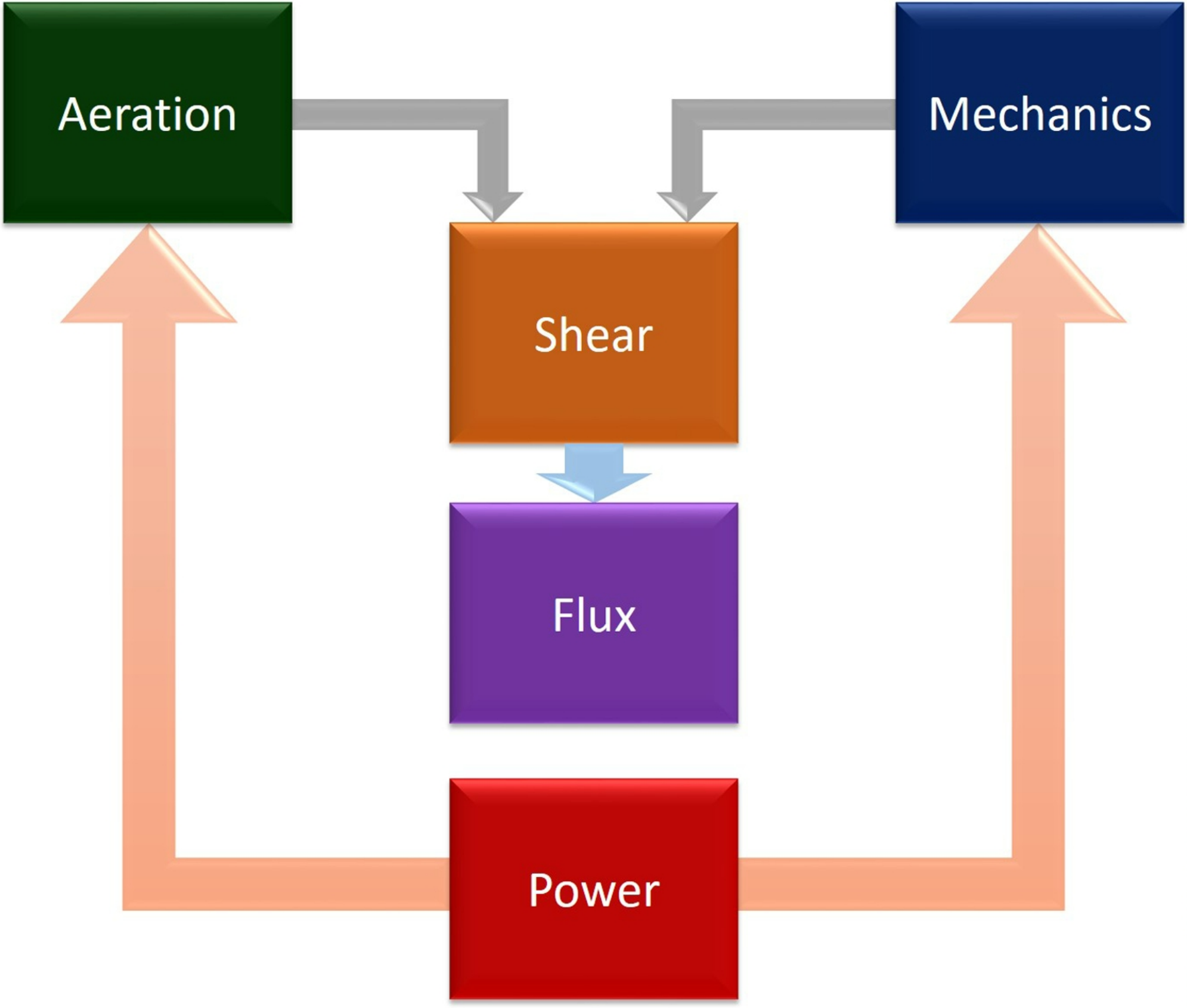
Aeration
Mechanics
Shear
Flux
Power

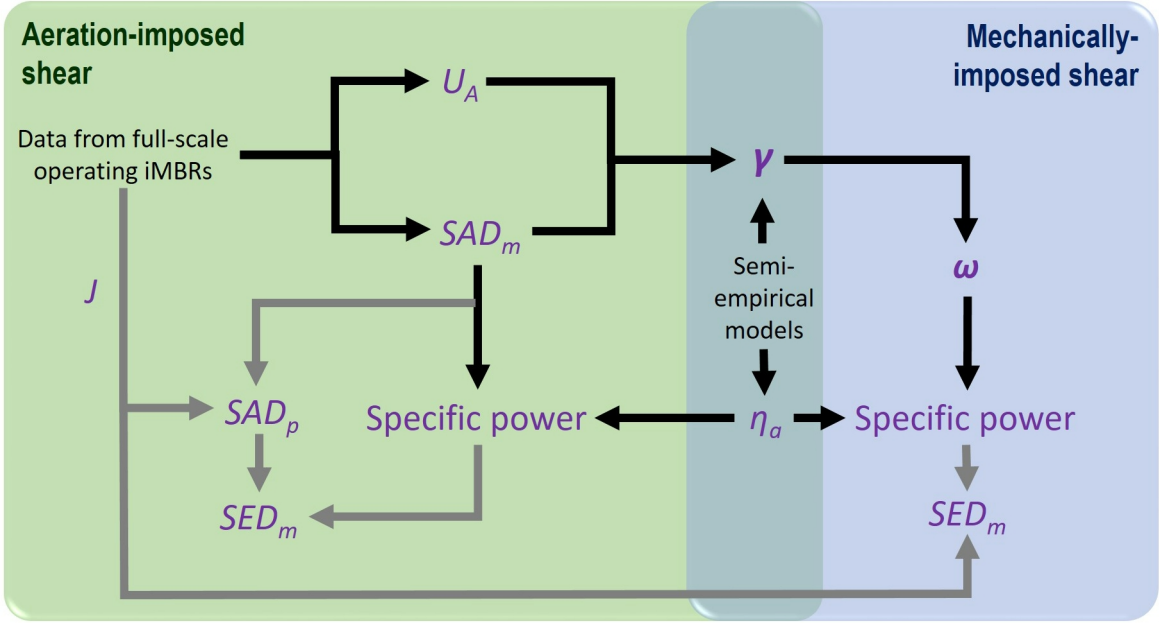
Aeration-imposed shear
Mechanically-imposed shear
Data from full-scale operating iMBRs
U_A
SAD_m
γ
ω
Semi-empirical models
J
SAD_p
Specific power
η_a
Specific power
SED_m
SED_m

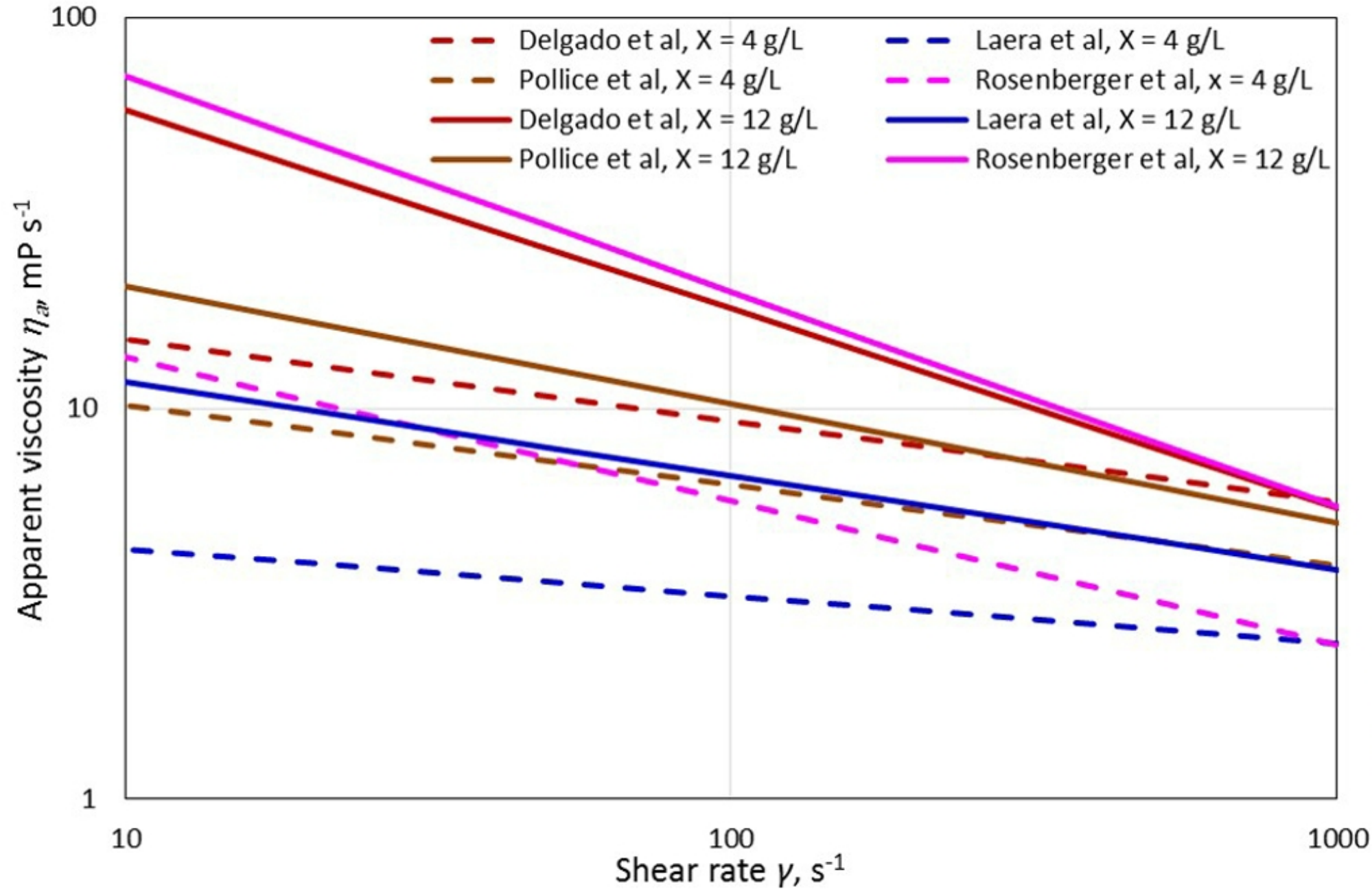
Delgado et al, X = 4 g/L
Pollice et al, X = 4 g/L
Delgado et al, X = 12 g/L
Pollice et al, X = 12 g/L
Laera et al, X = 4 g/L
Rosenberger et al, x = 4 g/L
Laera et al, X = 12 g/L
Rosenberger et al, X = 12 g/L
Apparent viscosity η_a, mP s^{-1}
100
10
1
10
100
1000
Shear rate γ, s^{-1}

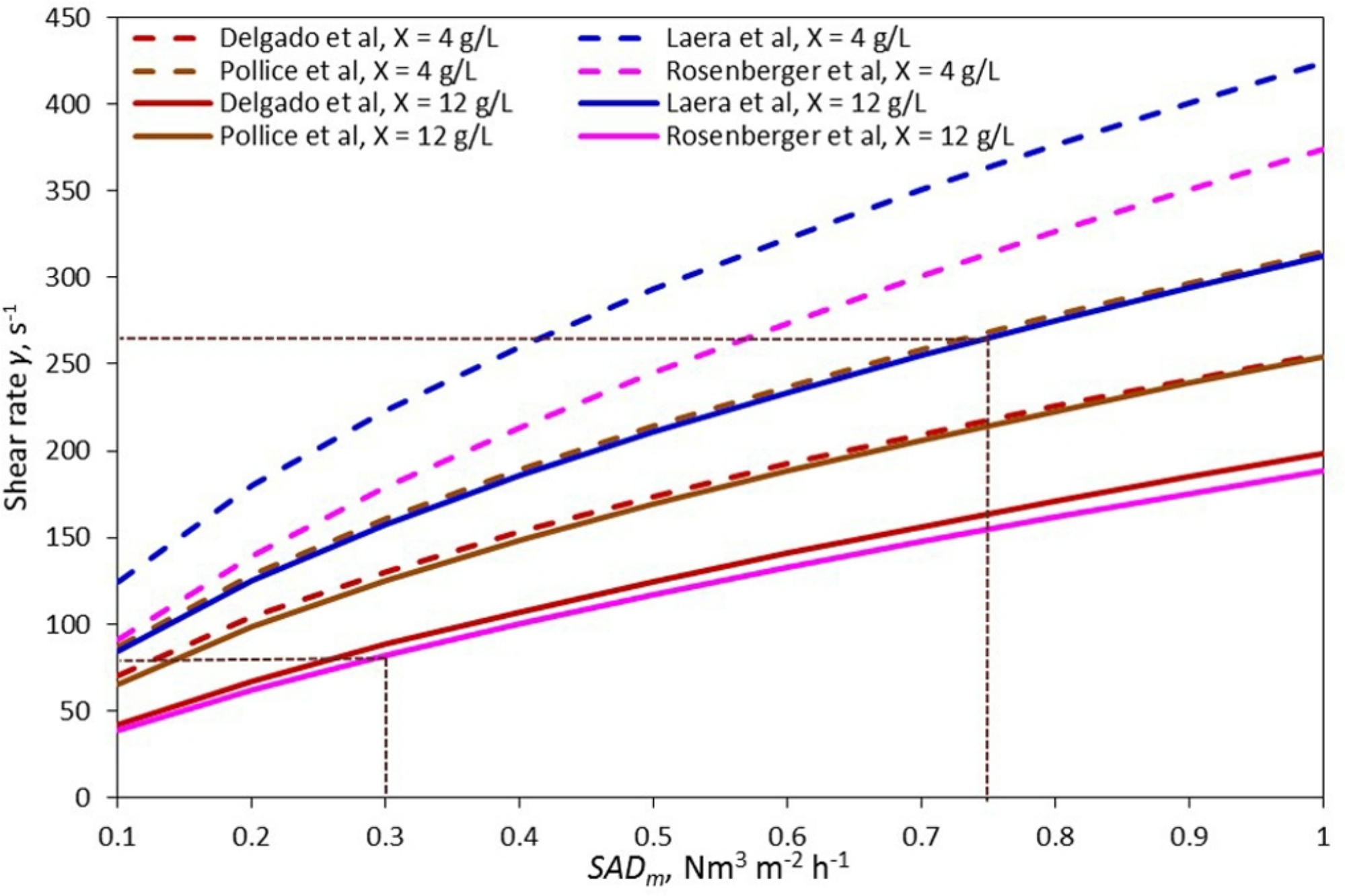
Delgado et al, X = 4 g/L
Pollice et al, X = 4 g/L
Delgado et al, X = 12 g/L
Pollice et al, X = 12 g/L
Laera et al, X = 4 g/L
Rosenberger et al, X = 4 g/L
Laera et al, X = 12 g/L
Rosenberger et al, X = 12 g/L
Shear rate γ, s-1
450
400
350
300
250
200
150
100
50
0
0.1
0.2
0.3
0.4
0.5
0.6
0.7
0.8
0.9
1
SADm, Nm3 m-2 h-1

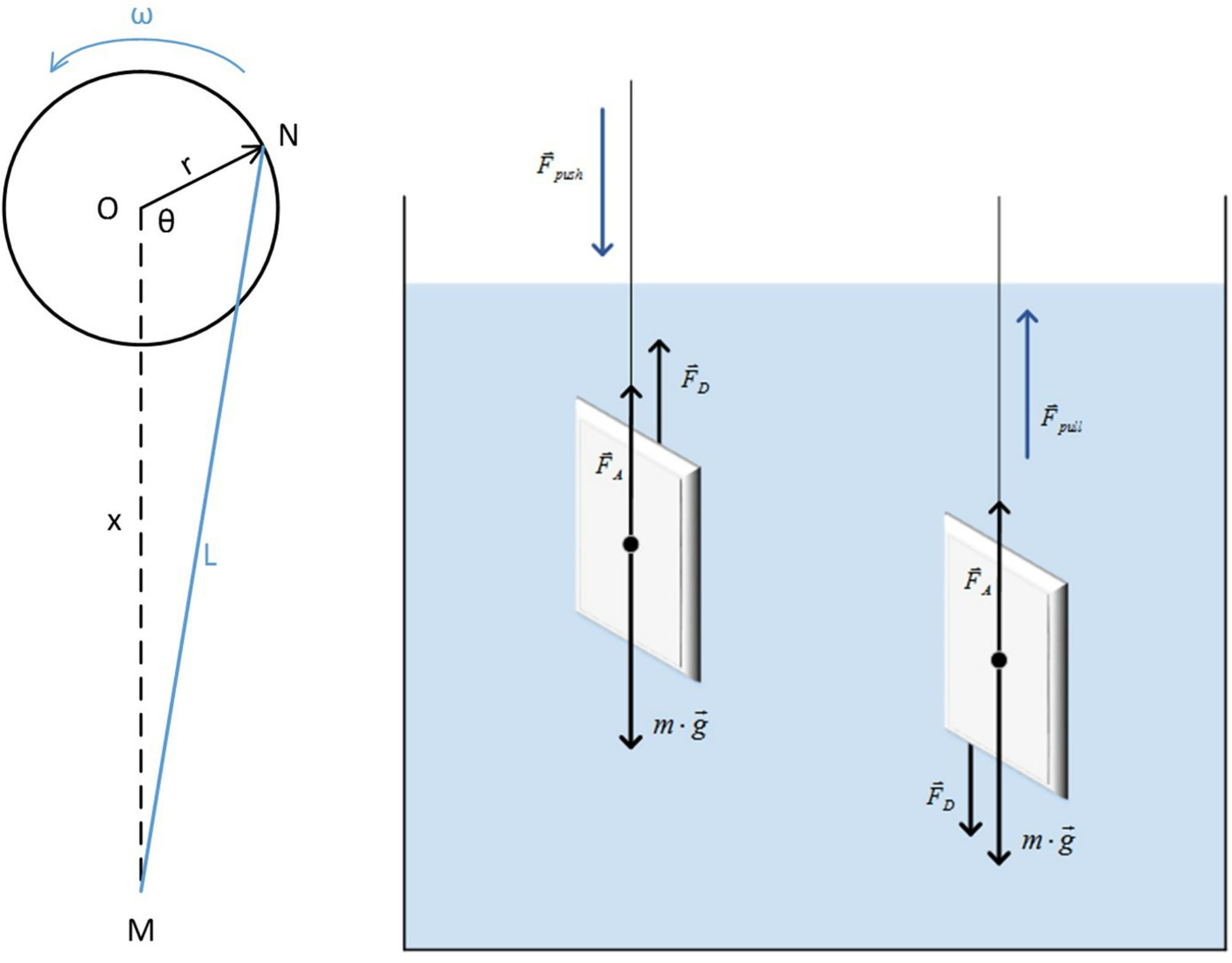
ω
N
r
O
θ
x
L
M
$\vec{F}_{push}$
$\vec{F}_D$
$\vec{F}_A$
$m \cdot \vec{g}$
$\vec{F}_{pull}$
$\vec{F}_A$
$\vec{F}_D$
$m \cdot \vec{g}$

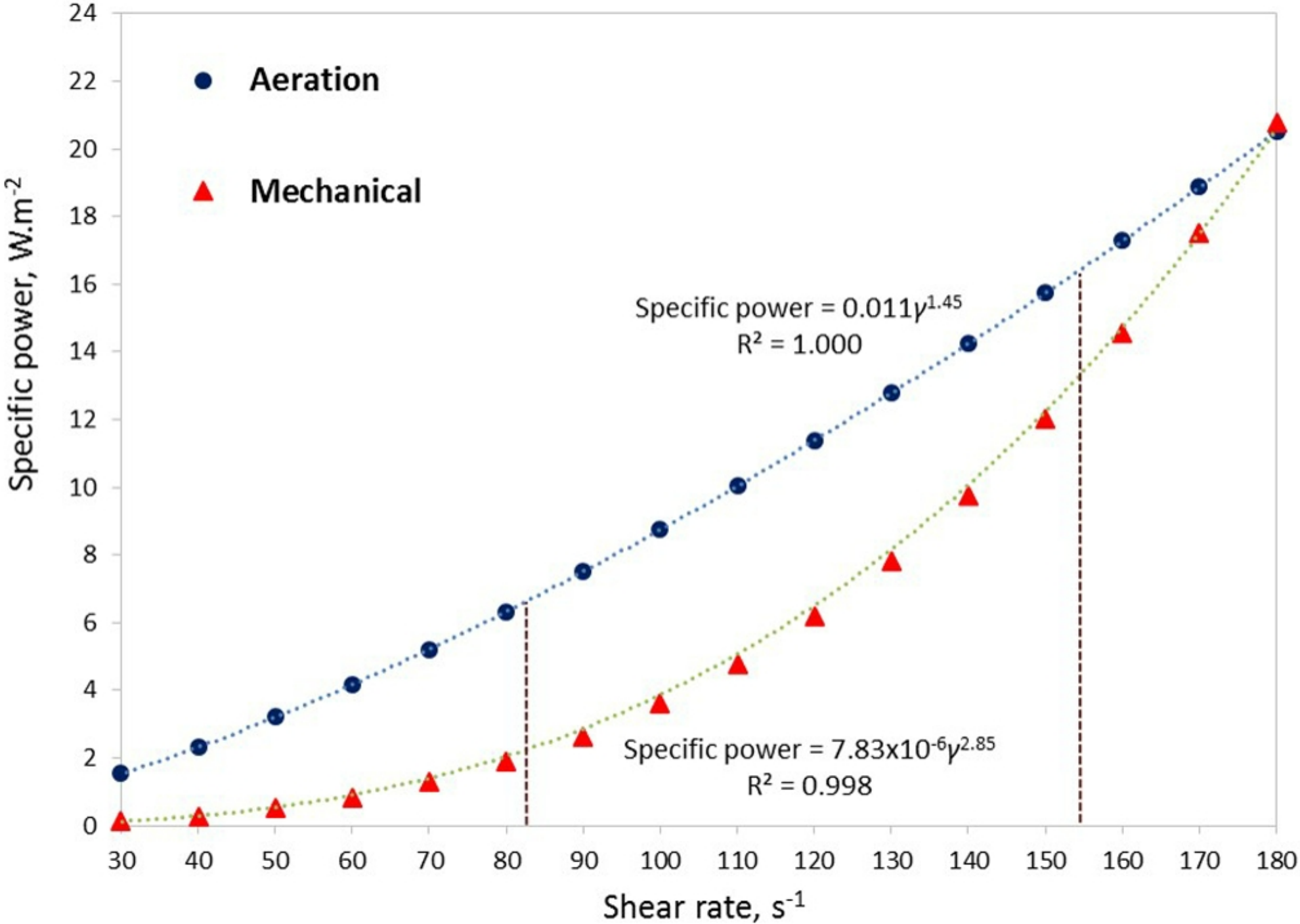
Aeration
Mechanical
Specific power = 0.011γ^1.45
R² = 1.000
Specific power = 7.83x10^-6γ^2.85
R² = 0.998
Specific power, W.m^-2
Shear rate, s^-1
0
2
4
6
8
10
12
14
16
18
20
22
24
30
40
50
60
70
80
90
100
110
120
130
140
150
160
170
180

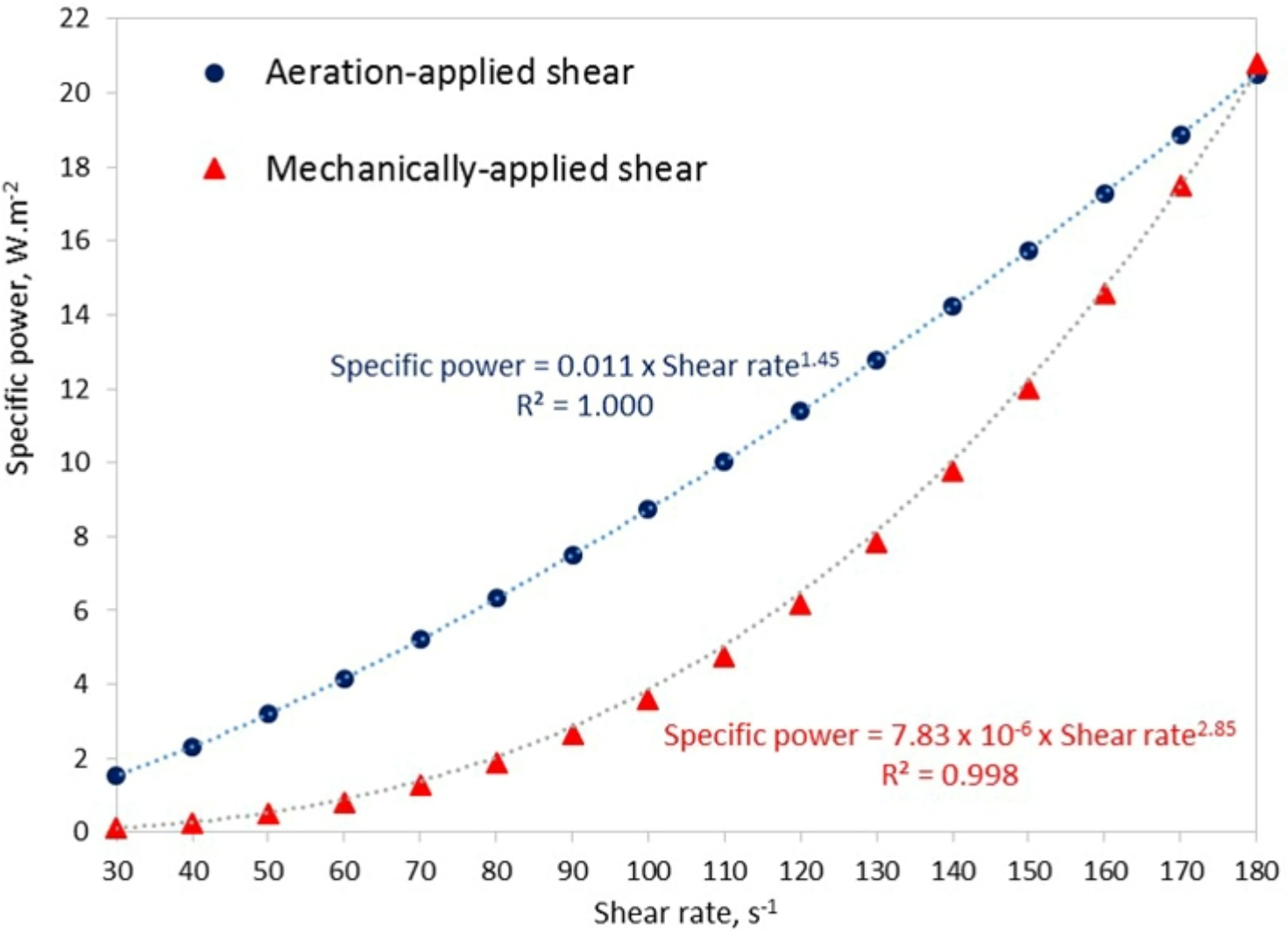
Aeration-applied shear
Mechanically-applied shear
Specific power = 0.011 x Shear rate^1.45
R² = 1.000
Specific power = 7.83 x 10^-6 x Shear rate^2.85
R² = 0.998
Specific power, W.m^-2
Shear rate, s^-1
0
2
4
6
8
10
12
14
16
18
20
22
30
40
50
60
70
80
90
100
110
120
130
140
150
160
170
180

Tables, Buzatu et al, WR39883

Table 1: Published values of empirical constants for Equation 1

Reference	**a**	**b**	**c**	**d**	MLSS range g L^{-1}	γ range s^{-1}	η_a range mPa s
Delgado et al, 2008	1.71	0.45	-0.068	0.81	5-14	20-130	15-76
Laera et al, 2007	0.882	0.494	-0.05	0.631	4-23	20-750	4-20
Pollice et al, 2006	1.94	0.262	-0.124	0.359	8-29	49-729	5-20
Rosenberger et al, 2002	1.9	0.43	-0.22	0.37	10-46	20-2200	20-800

Table 2: Published values of shear rate and interstitial air velocities for iMBRs

Reference	Config.	γ, s^{-1}	v_a, $m \cdot s^{-1}$
Yang et al, 2017	FS	116-175	0.053-0.106
Böhm and Kraume, 2015	FS	500-1500*	0.03-0.15*
Delgado et al, 2008	HF	18-132	-
Verrecht et al, 2008	FS & HF	-	0.037-0.109
Laera et al, 2007	HF	50-730	-

*Channel width (δ) dependent

Table 3: Operating conditions and outputs of aerated and mechanical shear comparison (Ho et al, 2015ab)

Parameter	*Unit*	*Aerated*	*Mechanical*
Design and operation			
Membrane area	m^2	50	45
Membrane length	m	2	1.3
TMP	kPa	20	<20
SAD_m	$Nm^3 \cdot m^{-2} \cdot h^{-1}$	0.2	-
Amplitude	mm	-	38-57
Reciprocation frequency	Hz	-	0.38-0.53
	RPM	-	23-32
Power	W	103	54-112
Specific power $\overline{P'}$, theoretical[a]	$W \cdot m^{-2}$	2.59	1.55
Experimental outputs			
Flux range	$L \cdot m^{-2} \cdot h^{-1}$ or LMH	20-24	20-40
Specific power[a] $\overline{P'}$	$W \cdot m^{-2}$	2.06	1.2-2.5
Specific power[a]	$kW \cdot bar \cdot LMH^{-1}$	0.8-1.7	0.19-0.83
Permeability	$LMH \cdot bar^{-1}$	60-120	200-300
SED, range at 20 LMH flux	$kWh \cdot m^{-3}$	0.11-0.14	0.04-0.09
SED, optimum	$kWh \cdot m^{-3}$	0.19[b]	0.064[b]
Efficiency (motor or blower)		40-65%	71%

[a]Corrected for optimum motor or blower efficiency
[b]Refers to maximum flux sustained experimentally